Math. Model. Nat. Phenom. 18 (2023) 1
https://doi.org/10.1051/mmnp/2022046

Mathematical Modelling of Natural Phenomena
www.mmnp-journal.org

MODELS OF RECRYSTALLIZATION ACTIVATED BY A DIFFUSION FLOW OF IMPURITIES FROM A THIN-FILM COATING WITH A CONVECTION TERM AT THE CRYSTAL SURFACE: EXACT SOLUTIONS

Sergey Savotchenko[1,*] and Aleksei Cherniakov[2]

Abstract. Two models of recrystallization are proposed taking into account the convective flux of impurity exchange between the polycrystalline and the thin-film coating. The special boundary modes of recrystallization described by the single-phase and two-phase Stefan problems with the boundary condition at coated surface containing the convective term. The exact solutions of the formulated problems corresponding to the grain-boundary concentration of impurities are obtained. The detail theoretical analysis focused on the third type problem shows that the concentration of impurities and the width of the recrystallized layer increase with an increase in the annealing time. An increase in intensity of impurity exchange between the polycrystalline and the coating promotes an increase in the width of the recrystallized layer. The recrystallization front position increases with an increase in the surface concentration of impurities and it decreases with an increase in the intensity of the impurity flux from the surface. The rate of recrystallization kinetics increases with an increase in the intensity of impurity exchange between the polycrystalline and the coating.

Mathematics Subject Classification. 82C70.

Received June 7, 2022. Accepted October 21, 2022.

1. Introduction

In order to describe theoretically the phase transitions in solids the heat (diffusion) equation with boundary condition at moving boundary is used often [1]. The moving boundary corresponds to the interface between two phases (phase transition boundary). The problem with unknown time dependence of the motion of the phase transition boundary usually represents the Stefan problem [27]. Various versions of Stefan's problem are well understood mathematically [28, 40, 43].

Even though such problems have become widely used to simulate processes caused by heat transfer [6, 44, 46], the formulation of problems for describing diffusion-controlled processes in polycrystalline solids can be considered insufficiently studied [23, 26]. Problems with moving boundaries acquire particular importance in the theoretical description of the kinetic regularities of recrystallization of metals and welds under the influence

Keywords and phrases: Diffusion equation, diffusion coefficient, Stefan problem, moving boundary, diffusion flow, convective term.

[1] Belgorod State Technological University named after V. G. Shukhov, 308012, Kostukova St., 46, Belgorod, Russia.
[2] Financial University Under the Government of the Russian Federation 125167, Leningradsky Pr., 49, Moscow, Russia.

[*] Corresponding author: savotchenkose@mail.ru

of a flux of impurity atoms from a thin-film coating applied to the surface [33, 37]. The kinetics of diffusion-controlled processes has been experimentally studied in a wide range of metal-coating systems [15, 22, 25]. It was found experimentally that the motion of the boundary of the recrystallized layer activated by the rest of the impurities obeys the root dependence on the annealing time [3, 20, 21]. The penetration of impurities from the coating occurs through grain boundary diffusion [13, 30, 31]. The penetration depth of impurities determines the width of the recrystallized layer in the case of their low solubility in the sample matrix [2, 14].

Of interest is a theoretical description of the regularities of recrystallization at various boundary regimes [10, 39, 45] for controlling the fluxes of impurities from the coating to the sample [8, 18, 19]. In the present paper, we describe the peculiarities of recrystallization kinetics activated by diffusion taking into account the impurity exchange between the polycrystalline and the coating. We consider two cases. The first one is the case of poorly soluble impurities in the matrix of the polycrystalline sample modeled by single-phase Stefan problem [17]. The second one describes the impurity penetration behind the recrystallization front modeled by two-phase Stefan problem [5, 34]. Here we focus on analysis on the third type problem in both cases. Note that the second type condition at fixed boundary corresponding to the sample surface was applied recently to theoretical description of recrystallization kinetics [32]. Recently we also propose the new diffusion models [35, 36].

Note that the various transfer processes used in different technical applications can be described theoretically by the diffusion/heat equation with the condition at the moving boundary. In particular, impurity segregation in the crystallization of melt is modeled numerically [38]. The authors of [12] study the segregation during silicon and germanium growth from thin melt layers using the submerged heater method with numeric simulation. The solidification of metals and melt crystallization are investigated for a long time [4, 41]. Recent papers [11, 42] report the results of modeling thermal conductivity. The authors of [9] investigated the longitudinal lattice temperature distribution of the active region and compared the thermal properties of metal-metal and semi-insulating surface-plasmon THz optical waveguides using a heat diffusion model. Features of crystallization kinetics at laser-powder cladding were actively investigated numerically [7, 16, 29]. New model of thermal behavior and solidification characteristics during laser welding of dissimilar metals was proposed in [24].

2. Single-phase model

2.1. Problem formulation

In this section, we propose the modified model of recrystallization of a polycrystal coated with a thin film of a material, which is poorly soluble in the matrix of the polycrystalline sample (*e.g.*, Ni in Mo or W [14, 20, 30]). The recrystallization is considered as the phase transition and the recrystallization front defines the phase transition boundary separating the recrystallized region and non-recrystallized one. The saturation of the material with impurities occurs only due to grain-boundary diffusion, since the rate of bulk diffusion is much lower than the rate of movement of the recrystallization front at the temperature at the beginning of recrystallization activation [22].

In the case of an impurity with very low solubility in the matrix of a polycrystalline sample, the width of recrystallized region is determined by the penetration of impurities into the depth of the sample along the grain boundaries. Therefore, the single-phase model of recrystallization can be applied.

We consider the system geometry as was described in [32]. The x axis perpendicular to the flat surface of a semi-infinite polycrystalline sample, and a thin-film coating is placed in the yz plane. It is supposed that the diffusion of impurities (diffusant) occurs into polycrystalline sample from the surface ($x = 0$) in depth uniformly over its, and the position of the moving recrystallization front is the function of time $x_b(t)$, which is determined experimentally usually as $x_b(t) \sim t^{1/2}$ [22]. Thus, in order to find exact explicit expression of distribution of impurity concentration along the grain boundary, we formulate the model of recrystallization using the problem with moving boundary (the Stefan problem) [27].

In the case considered, the concentration $u(x,\ t)$ into the grain boundary is determined as a solution of non-stationary diffusion equation

$$\frac{\partial u}{\partial t} = \frac{\partial}{\partial x}\left(D(x)\frac{\partial u}{\partial x}\right), \tag{2.1}$$

with the diffusion coefficient defined by the stepwise function

$$D(x) = \begin{cases} D_1,\ 0 < x < x_b(t) \\ 0,\ x > x_b(t) \end{cases}$$

where D_1 is the grain boundary diffusion coefficient at the recrystallized region.

The impurity concentration at the moving boundary of the recrystallization front at $x = x_b(t)$ assumed to be negligible. Then, we can write the following condition at the moving boundary

$$u|_{x=x_b} = 0. \tag{2.2}$$

The diffusion flux through the recrystallization front is proportional to the velocity of the recrystallization front on this moving boundary. Then, we can use the Stefan condition at the moving boundary

$$D_1\left(\frac{\partial u}{\partial x}\right)\bigg|_{x=x_b} = -\gamma\frac{\mathrm{d}x_b}{\mathrm{d}t}, \tag{2.3}$$

where γ is a known positive constant.

The diffusion flow of impurities from a thin-film coating at the sample surface $x = 0$ is given by

$$j_0 = -D_1\left(\frac{\partial u}{\partial x}\right)\bigg|_{x=0}. \tag{2.4}$$

We take into account the possibility of convective outflow of diffusant at the surface with a thin-film coating. We suppose that the diffusant flow is proportional to the difference between the diffusant concentration at the surface $u|_{x=0}$ and concentration of the constant diffusant outflow u_s. Therefore, the diffusant flow can be written as

$$j_0 = -\alpha(u|_{x=0} - u_s). \tag{2.5}$$

The value of α characterizes intensity of impurity exchange between the polycrystalline and the coating. It is defined as the flux of diffusant from a unit of surface area per unit of time with a difference in the concentration of impurities between the surface and the coating of one unit.

Equating flows (2.4) and (2.5), we obtain the boundary condition at the surface

$$\left(\alpha u - D_1\frac{\partial u}{\partial x}\right)\bigg|_{x=0} = \alpha u_s. \tag{2.6}$$

The condition with convective term (2.6) is the boundary condition of the third type. Thus, the grain boundary concentration is the solution of diffusion equation (2.1) satisfying the boundary conditions (2.2) and (2.3) at the moving boundary (phase transition boundary) and the condition (2.6) of the third type at the fixed boundary (surface). The solution of the problem formulated must be a continuous, finite and decreasing function of x.

In order to find exact solution of problem we consider the general case consisting of the conditions at the fixed boundary of the first type

$$u\big|_{x=0} = u_s, \tag{2.7}$$

the second type

$$D_1 \left(\frac{\partial u}{\partial x}\right)\bigg|_{x=0} = -\alpha u_s. \tag{2.8}$$

and the third type (2.6).

For this, we write the general condition at the fixed boundary as follows:

$$\left(\sigma_1 u - \sigma_2 \frac{D_1}{\alpha}\frac{\partial u}{\partial x}\right)\bigg|_{x=0} = u_s, \tag{2.9}$$

where we introduce indicators $\sigma_{1,2}$. In the case of $\sigma_1 = 1$ and $\sigma_2 = 0$ condition (2.9) transforms into boundary condition of the first type (2.7); in the case of $\sigma_1 = 0$ and $\sigma_2 = 1$ condition (2.9) transforms into boundary condition of the second type (2.8); in the case of $\sigma_1 = 1$ and $\sigma_2 = 1$ condition (2.9) transforms into boundary condition of the third type (2.6).

As well known, the exact solutions of the Stefan problems with boundary condition of the second and the third types exist when the concentration flux of impurities $\sim t^{1/2}$ is maintained on the sample surface. The assumption about the possibility of using the root dependence on time is justified by the fact that many processes are described precisely by the root dependence on time, which makes it common in analytical calculations. Then, in order to obtain exact solution of the problem, we put below $D_1/\alpha = h(\pi D_1 t)^{1/2}$, where h is a constant determined by the intensity of the impurity flux from the surface.

2.2. Exact solutions

As well known, the solution to diffusion equation (2.1) with constant diffusion coefficient $D = D_1$ at $0 < x < x_b(t)$ can be presented as $u(x,t) = A + B\mathrm{erf}(x/2\sqrt{D_1 t})$, where constants A and B are found from the boundary conditions. Substituting this solution into the boundary conditions (2.2), (2.3) and (2.9) (we emphasize that it is necessary to replace D_1/α with $h(\pi D_1 t)^{1/2}$ in equation (2.9) in order to obtain exact solution of the problem), we find that the exact solution to diffusion equation (2.1) satisfying the boundary conditions (2.2), (2.3) and (2.9) in general form can be written as

$$u(x,t) = u_s \frac{\mathrm{erf}(\beta) - \mathrm{erf}(x/2\sqrt{D_1 t})}{\sigma_1 \mathrm{erf}(\beta) + \sigma_2 h}, \tag{2.10}$$

where $\mathrm{erf}(z) = \dfrac{2}{\sqrt{\pi}} \int_0^z e^{-y^2}\mathrm{d}y$ is the error function, β is the positive root of equation (we denote below $k = u_s/\gamma\sqrt{\pi}$):

$$\beta e^{\beta^2}(\sigma_1 \mathrm{erf}(\beta) + \sigma_2 h) = k, \tag{2.11}$$

which defines the moving recrystallization front position as follows

$$x_b(t) = 2\beta\sqrt{D_1 t}. \tag{2.12}$$

The solution (2.10) and equation (2.11) of general problem allows to write:

i) the solution of the firs type problem, which satisfies the boundary condition of the first type (2.7) at the surface [37], as follows

$$u(x,t) = u_s \left\{ 1 - \frac{\mathrm{erf}(x/2\sqrt{D_1 t})}{\mathrm{erf}(\beta)} \right\}, \tag{2.13}$$

where

$$\beta e^{\beta^2} \mathrm{erf}(\beta) = k; \tag{2.14}$$

ii) the solution of the second type problem, which satisfies the boundary condition of the second type (2.8) at the surface, as follows

$$u(x,t) = u_s \{\mathrm{erf}(\beta) - \mathrm{erf}(x/2\sqrt{D_1 t})\}/h, \tag{2.15}$$

$$\beta e^{\beta^2} = k/h; \tag{2.16}$$

iii) the solution of the third type problem, which satisfies the boundary condition of the third type (2.6) at the surface, as follows

$$u(x,t) = u_s \frac{\mathrm{erf}(\beta) - \mathrm{erf}(x/2\sqrt{D_1 t})}{\mathrm{erf}(\beta) + h}, \tag{2.17}$$

$$\beta e^{\beta^2} (\mathrm{erf}(\beta) + h) = k. \tag{2.18}$$

Typical dependences of the distribution of the grain-boundary concentration of impurities (2.17) in the recrystallized region at the fixed time in the case of third type problem are shown in Figure 1a. The impurity concentration decreases monotonically to zero value at the moving boundary of recrystallized layer x_b. The penetration depth decreases with an increasing h. Therefore, an increase in intensity of impurity exchange between the polycrystalline and the coating promotes an increase in the width of the recrystallized layer.

Typical dependence of impurity concentration on annealing time (2.17) at fixed distance from the sample surface in the case of third type problem is shown in Figure 1b. The concentration increases monotonically over time reaching the saturation value of $u_0 = u_s \mathrm{erf}(\beta)/(\mathrm{erf}(\beta) + h)$.

2.3. Analysis of the recrystallization front kinetics

The kinetics of recrystallization front is determined by equation (2.12). The position of recrystallization front versus $t^{1/2}$ is the straight line with an angle of inclination determined by parameter β. It determines the rate of recrystallization kinetics. The transcendental equation (2.11) can be solved in general case numerically only. We focus below on the case of the third type problem.

The results of numerical analysis of equation (2.18) are presented in Figure 2. Note that the numerical solutions to equation (2.18) can be easy obtained from the explicit function $h = k/\beta e^{-\beta^2} - \mathrm{erf}(\beta)$, which we inverse and then plot the dependence $\beta = \beta(h)$. Figure 2a demonstrates the typical dependencies of equation (2.18) root β on characteristic parameter of the third type problem h. The calculations show that β monotonically decreases with an increase in h. Figure 2b demonstrates the typical dependence of kinetics of recrystallization front position (2.12) calculated with root of equation (2.18) on h. Typical dependences of the moving recrystallization front position (2.12) calculated with roots of equation (2.18) are shown in Figure 2c. An increase in h leads to a decrease in penetration depth of impurities. Hence, the rate of recrystallization kinetics increases

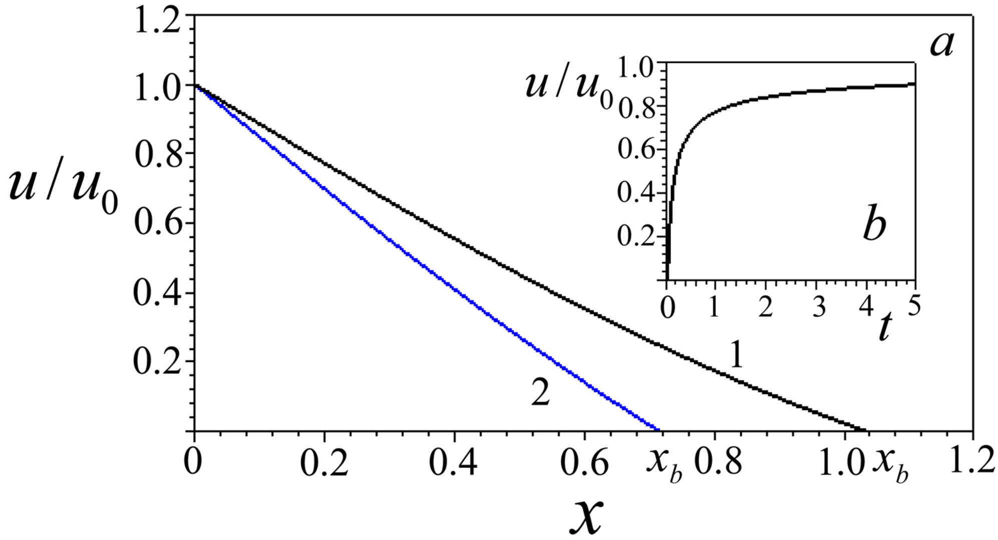

FIGURE 1. The concentration distribution (2.17) along the x-axis (a) with $D_1 = 0.5$; $t = 1$; $k = 1$; $h = 0.5$ (line 1) and $h = 1$ (line 2); kinetic dependencies of concentration (b) with $h = 0.5$; $x = 0.2$ (in conventional units).

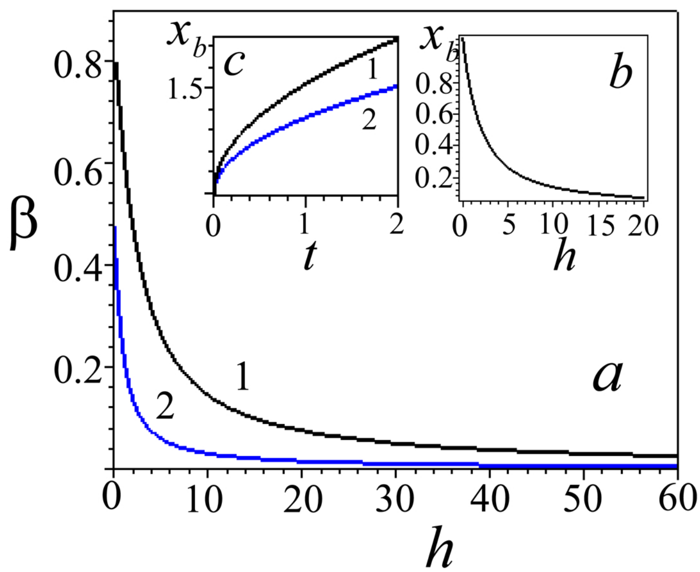

FIGURE 2. Dependencies on h of roots of equation (2.18) with $k = 1.5$ (line 1) and $k = 0.3$ (line 2) (a); the position of recrystallization front (b) defined by (2.12) and root of equation (2.18) with $D_1 = 0.5$; $t = 1$; $k = 1$; the kinetic dependencies of the position of recrystallization front (c) with $h = 0.5$ (line 1) and $h = 1$ (line 2) (in conventional units).

with an increase in the intensity of impurity exchange between the polycrystalline and the coating. An increase in k promotes an increase in β. Therefore, the rate of crystallization kinetics increases with an increase in the surface concentration u_s and with a decrease in γ.

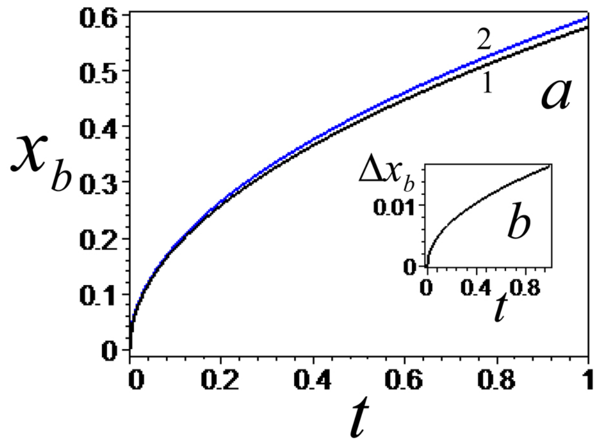

FIGURE 3. Kinetic dependencies $x_b(t)$ calculated from equation (2.12) with exact root of equation (2.14) (line 1) and $x_b(t)$ calculated from approximate equation (2.21) (line 2) (a), and the absolute difference Δx_b between these exact and approximate solutions (b) with $k = 0.1$, $D_1 = 1$.

The solution of transcendent equation (2.11) can be solved analytically in the case of small values of the parameter β. In this case of $\beta \ll 1$ we can put in equation (2.11) $\exp(\beta^2) \sim 1$ and $\mathrm{erf}(\beta) \approx 2\beta/\sqrt{\pi}$, then we get the equation

$$2\beta^2\sigma_1/\sqrt{\pi} + \beta\sigma_2 h - k = 0, \tag{2.19}$$

the positive root of which is given by

$$\beta = \sqrt{\pi}\{\sqrt{(\sigma_2 h)^2 + 8\sigma_1 k/\sqrt{\pi}} - \sigma_2 h\}/4\sigma_1. \tag{2.20}$$

In the case of the boundary condition of the first type (2.7) from equation (2.19) we find $\beta = (u_s/2\gamma)^{1/2}$, which can be obtained directly from equation (2.14). Then, the dependence of the position of the recrystallization front (2.12) takes the form

$$x_b(t) = (2u_s D_1 t/\gamma)^{1/2}. \tag{2.21}$$

The recrystallization front position (2.21) increases with an increase in the surface concentration of impurities, and it decreases with increasing parameter γ of Stefan condition.

In order to demonstrate the comparison of exact analytical and approximate solutions, we plot in Figure 3a kinetic dependencies $x_b(t)$ calculated from equation (2.12) with exact root of equation (2.14) and $x_b(t)$ calculated from approximate equation (2.21). Figure 3b demonstrates the absolute difference Δx_b between these exact and approximate solutions. We find that the absolute difference Δx_b is very small (about 0.001–0.016 at $0 < t < 1$) and the relatively difference $\Delta x_b/x_b$ is about 2.8% at $0 < t < 1$. This indicates a good accuracy of the approximate equation (2.21) for small values of k.

Approximate expression (2.21) allows simple estimating the depth of diffusant penetration into the polycrystalline during annealing with known surface concentration of impurities and the coefficient of grain-boundary diffusion [37]. From experiments of nickel grain-boundary diffusion in molybdenum an approximate estimate of the recrystallized layer depth in pre-deformed molybdenum gives a value about $x_b \approx 158$, μm,according with equation (2.21) after 10 h of annealing with $D_1 = 10^{-12}$ m^2/s [20–22], and $\gamma = 1.44$ and the nickel concentration on the surface $u_s = 50\%$. Note that the calculation of position of recrystallization front (2.12) with exact root β of equation (2.14) with the same values of diffusion parameters gives the value about 150 µm. The obtained estimations of penetration depth of nickel in molybdenum are in satisfactory agreement with the experimental data [14, 20–22].

In the case of the boundary condition of the second type (2.8) from equation (2.19) we find $\beta = k/h$, which can be obtained directly from equation (2.16). Then, the dependence of the position of the recrystallization front (2.12) takes the form

$$x_b(t) = (2u_s/\gamma h)\sqrt{D_1 t/\pi}. \tag{2.22}$$

The recrystallization front position (2.22) decreases with an increase in the intensity of the impurity flux from the surface.

In the case of the boundary condition of the third type (2.6) from equation (2.19) we find

$$\beta = \beta_1(\sqrt{1 + (\beta_2/\beta_1)^2} - 1), \tag{2.23}$$

where $\beta_1 = h\sqrt{\pi}/4$ and $\beta_2^2 = k\sqrt{\pi}/2$. The recrystallization front position defined by root (2.23) increases with an increase in intensity of impurity exchange between the polycrystal and the coating. The smallness of the β defined by equation (2.23) is ensured by the fulfillment of the condition $h \ll 1$ or $k \ll h$.

3. Two-phase model

3.1. Problem formulation

Here we consider the modified two-phase model of activated recrystallization [33]. This model is used in the case when the diffusant can penetrate behind the recrystallization front. In this case, the penetration depth of the diffusant will be greater than the width of the recrystallized layer. Then the concentration of diffusant after the recrystallization front at $x > x_b(t)$ cannot be considered negligible although the concentration at the region $0 < x < x_b(t)$ before the phase transition boundary $x_b(t)$ is greater than the concentration after the phase transition boundary $x_b(t)$ at the region $x > x_b(t)$. It is necessary to take into account the distribution of the diffusant after the recrystallization front at $x > x_b(t)$.

The system geometry is the same as in Section 2. The diffusion coefficient in equation (2.1) is given now by

$$D(x) = \begin{cases} D_1, \ 0 < x < x_b(t) \\ D_2, \ x > x_b(t) \end{cases} \tag{3.1}$$

where $D_{1,2}$ are the known positive constants.

The initial condition is specified in the two-phase Stefan problem:

$$u|_{t=0} = u_0, \tag{3.2}$$

where u_0 is known impurity concentration of at initial moment of time $t = 0$.

We suppose that the impurity concentrations of both phases are the same at the moving boundary:

$$u|_{x=x_b-0} = u|_{x=x_b+0} = u_b, \tag{3.3}$$

where u_b is known impurity concentration of at the moving boundary (the phase transition concentration).

The diffusion flow through the recrystallization front suffers a jump proportional to the speed of its movement that it can be written with using the standard Stefan condition at the moving boundary:

$$D_2 \left(\frac{\partial u}{\partial x} \right) \Big|_{x=x_s+0} - D_1 \left(\frac{\partial u}{\partial x} \right) \Big|_{x=x_s-0} = \gamma \frac{\mathrm{d}x_s}{\mathrm{d}t}. \tag{3.4}$$

The condition at the fixed boundary is defined by the same equation (2.9), which can be rewritten as follows

$$\left(\sigma_1 u - \sigma_2 h \sqrt{\pi D_1 t} \frac{\partial u}{\partial x} \right) \Big|_{x=0} = u_s, \tag{3.5}$$

Thus, the two-phase model of recrystallization is an initial-boundary value problem (2.1), (3.1)–(3.5). The detail analysis we hold in [32] in the case of the problem of the second type. We focus below on analysis of the problem of the third type.

3.2. Exact solutions

As well known, the solution to diffusion equation (2.1) with diffusion coefficient defined by equation (3.1) can be presented as

$$u(x,t) = \begin{cases} A_1 + B_1 \mathrm{erf}(x/2\sqrt{D_1 t}), & 0 < x < x_b(t) \\ A_2 + B_2 \mathrm{erf}(x/2\sqrt{D_2 t}), & x > x_b(t) \end{cases}$$

where constants $A_{1,2}$ and $B_{1,2}$ are found from the boundary conditions. Substituting this solution into the boundary conditions (3.2)–(3.5), we find that the exact solution of the problem (2.1), (3.1)–(3.5) in general form is given by

$$u(x,t) = \begin{cases} u_b + \dfrac{u_s - u_b \sigma_1}{\sigma_1 \mathrm{erf}(\beta) + \sigma_2 h} \left\{ \mathrm{erf}(\beta) - \mathrm{erf}\left(\dfrac{x}{2\sqrt{D_1 t}} \right) \right\}, & 0 < x < x_b(t) \\ u_0 + (u_b - u_0) \dfrac{\mathrm{erfc}(x/2\sqrt{D_2 t})}{\mathrm{erfc}(\beta/\theta)}, & x > x_b(t) \end{cases} \tag{3.6}$$

where $\theta = \sqrt{D_2/D_1}$, $\mathrm{erfc}(z) = 1 - \mathrm{erf}(z)$, and the phase transition boundary is given by the same equation (2.12) with β defined by the positive root of equation

$$\frac{u_s - u_b \sigma_1}{\sigma_1 \mathrm{erf}(\beta) + \sigma_2 h} e^{-\beta^2} - \theta e^{-(\beta/\theta)^2} \frac{u_b - u_0}{\mathrm{erfc}(\beta/\theta)} = \sqrt{\pi} \beta \gamma. \tag{3.7}$$

The solution (3.6) and equation (3.7) of general problem allows to write:

i) the solution of the firs type problem, which satisfies the boundary condition of the first type (2.7) at the surface, as follows

$$u(x,t) = \begin{cases} u_b + (u_s - u_b) \left\{ 1 - \dfrac{\mathrm{erf}(x/2\sqrt{D_1 t})}{\mathrm{erf}(\beta)} \right\}, & 0 < x < x_b(t) \\ u_0 + (u_b - u_0) \dfrac{\mathrm{erfc}(x/2\sqrt{D_2 t})}{\mathrm{erfc}(\beta/\theta)}, & x > x_b(t) \end{cases}, \tag{3.8}$$

$$\frac{u_s - u_b}{\mathrm{erf}(\beta)} e^{-\beta^2} - \theta e^{-(\beta/\theta)^2} \frac{u_b - u_0}{\mathrm{erfc}(\beta/\theta)} = \sqrt{\pi} \beta \gamma; \tag{3.9}$$

ii) the solution of the second type problem, which satisfies the boundary condition of the second type (2.8) at the surface, as follows

$$u(x,t)=\left\{\begin{array}{l} u_b+u_s\{\mathrm{erf}(\beta)-\mathrm{erf}(x/2\sqrt{D_1 t})\}/h,\ \ 0<x<x_b(t) \\ u_0+(u_b-u_0)\dfrac{\mathrm{erfc}(x/2\sqrt{D_2 t})}{\mathrm{erfc}(\beta/\theta)},\ \ x>x_b(t) \end{array}\right. , \tag{3.10}$$

$$\frac{u_s}{h}e^{-\beta^2}-\theta e^{-(\beta/\theta)^2}\frac{u_b-u_0}{\mathrm{erfc}(\beta/\theta)}=\sqrt{\pi}\beta\gamma; \tag{3.11}$$

iii) the solution of the third type problem, which satisfies the boundary condition of the third type (2.6) at the surface, as follows

$$u(x,t)=\left\{\begin{array}{l} u_b+\dfrac{u_s-u_b}{\mathrm{erf}(\beta)+h}\left\{\mathrm{erf}(\beta)-\mathrm{erf}\left(\dfrac{x}{2\sqrt{D_1 t}}\right)\right\},\ \ 0<x<x_b(t) \\ u_0+(u_b-u_0)\dfrac{\mathrm{erfc}(x/2\sqrt{D_2 t})}{\mathrm{erfc}(\beta/\theta)},\ \ x>x_b(t) \end{array}\right. , \tag{3.12}$$

$$\frac{u_s-u_b}{\mathrm{erf}(\beta)+h}e^{-\beta^2}-\theta e^{-(\beta/\theta)^2}\frac{u_b-u_0}{\mathrm{erfc}(\beta/\theta)}=\sqrt{\pi}\beta\gamma. \tag{3.13}$$

Typical dependences of the distribution of the impurity grain-boundary concentration (3.12) in the recrystallized layer and ahead of the recrystallization front at the fixed time in the case of third type problem are shown in Figure 4. A flow jump at the boundary of the recrystallization front causes a non-smooth profile of the impurity concentration distribution. A decrease in h leads to the increase in impurity concentration at fixed distance from the sample surface (Fig. 4a). The impurity concentration in recrystallized layer ($x<x_b$) in the case of $D_1<D_2$ ($\theta>1$) is lower than in the case of $D_1>D_2$ ($\theta<1$) at the fixed time, and the concentration in non-recrystallized region ($x>x_b$) in the case of $D_1<D_2$ is higher than in the case of $D_1>D_2$ (Fig. 4b). The concentration of impurities and the width of the recrystallized layer increase with an increase in the annealing time (Fig. 4c).

3.3. Analysis of the recrystallization front kinetics

We mention above that the value of β completely determines the kinetics of the recrystallization front. The analysis showed that the values of the root of equation (3.7) significantly depend on the model parameters, and its positive values do not exist for all values of the parameters. The solution of equation (3.7) is a function of u_0, u_c, u_b, θ, γ and h. The transcendental equation (3.7) can be solved in general case numerically only.

However, the explicit analytical solution of equation (3.7) could be found in the case of small value of β. In the case of $\beta\ll 1$ equation (3.7) transforms into square equation

$$a\beta^2+b\beta+c=0, \tag{3.14}$$

where

$$a=(2\gamma-u_b)\sigma_1+u_s,$$

$$b=\sqrt{\pi}\gamma h\sigma_2+\frac{2}{\theta\sqrt{\pi}}\{u_s+\sigma_1[\theta^2(u_b-u_0)-u_b]\},$$

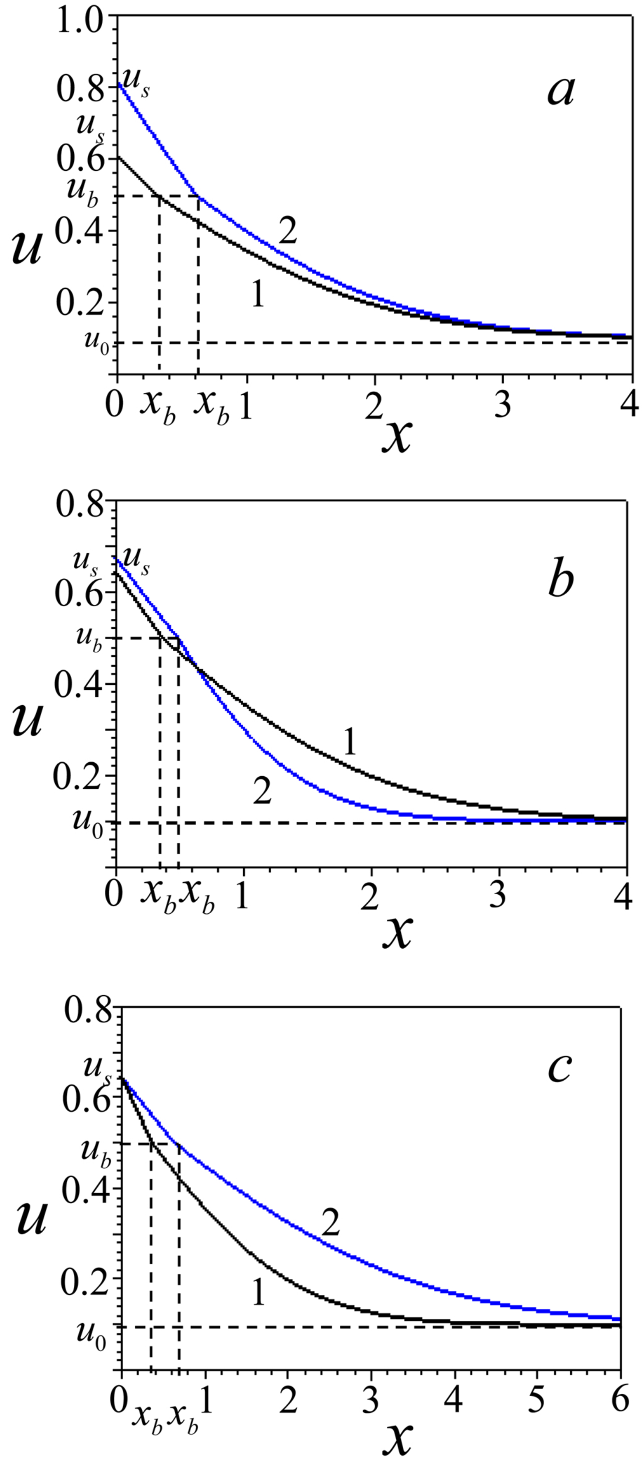

Figure 4. The concentration distribution (3.12) along the x-axis (a) with $D_1 = 1$; $u_s = 1$; $u_b = 0.5$; $u_0 = 0.1$; $\gamma = 0.5$ (in conventional units); (a) $-$ $\theta = 1.1$; $t = 1$; $h = 0.6$ (line 1) and $h = 0.2$ (line 2); (b) $-$ $h = 0.5$; $t = 1$; $\theta = 1.1$ (line 1) and $\theta = 0.7$ (line 2); (c) $-$ $\theta = 1.1$; $h = 0.5$; $t = 1$ (line 1) and $t = 3$ (line 2).

$$c = \sigma_2 h\theta(u_b - u_0) - (u_s - u_b\sigma_1).$$

Note that in the case of the second and the third type problems, the equation (3.14) becomes the linear one. The quadratic term in equation (3.14) is necessary only for the first type problem. In this case, the solution of equation (3.14) can be written as

$$\beta = \frac{\sqrt{D} - [u_s - u_b + \theta^2(u_b - u_0)]}{\sqrt{\pi}\theta(2\gamma + u_s - u_b)}, \tag{3.15}$$

where $D = [u_s - u_b + \theta^2(u_b - u_0)]^2 + \pi\theta^2(u_s - u_b)(2\gamma + u_s - u_b)$.

It is interesting to note that the solution of equation (3.14) exists in the case of $\gamma = 0$. This case is corresponding to the smooth concentration distribution [36].

It is sufficient to restrict oneself to a linear term in equation (3.14) in the case of the second boundary value problem and the solution is given by

$$\beta = \theta\sqrt{\pi}\frac{u_s - \theta h(u_b - u_0)}{\pi\gamma\theta h + 2u_s}. \tag{3.16}$$

In the case of the third boundary value problem, we restrict to a linear term in equation (3.14) too, and find the solution as follows

$$\beta = \theta\sqrt{\pi}\frac{u_s - u_b - \theta h(u_b - u_0)}{\pi\gamma\theta h + 2[u_s - u_b + \theta^2(u_b - u_0)]}. \tag{3.17}$$

In the case of small value of θ (this case corresponds to the condition of $D_2 \ll D_1$) from equation (3.17) we find the simplest estimation of the root as

$$\beta \approx \sqrt{\pi}\theta/2, \tag{3.18}$$

which allows to obtain the estimation of the recrystallization front position as

$$x_b(t) \approx \sqrt{\pi D_2 t}. \tag{3.19}$$

In the case of small value of h from equation (3.17) we find that the parameter β is linearly decreases with an increase in h as follows:

$$\beta \approx \beta_0 - \beta_1 h, \tag{3.20}$$

where

$$\beta_0 = \theta\sqrt{\pi}\frac{1}{1 + \theta^2\dfrac{u_b - u_0}{u_s - u_b}},$$

$$\beta_1 = \frac{\theta^2\sqrt{\pi}}{2[u_s - u_b + \theta^2(u_b - u_0)]}\left\{u_b - u_0 + \frac{\pi\gamma(u_s - u_b)}{2[u_s - u_b + \theta^2(u_b - u_0)]}\right\}.$$

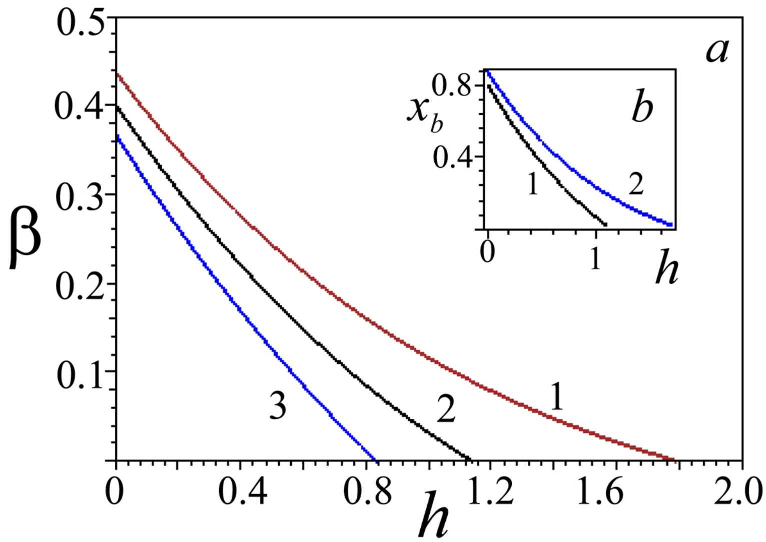

FIGURE 5. Dependencies on h of roots of equation (3.13) with $D_1 = 1$; $u_s = 1$; $u_b = 0.5$; $u_0 = 0.1$; $\gamma = 0.5$; (a) $\theta = 0.7$ (line 1); $\theta = 1.1$ (line 2); $\theta = 1.5$ (line 3) and the position of recrystallization front (b) defined by (2.12) and root of equation (3.13) with $t = 1$; $\theta = 1.1$ (line 1); $\theta = 0.7$ (line 2) (in conventional units).

We focus below on numerical analysis of kinetics of recrystallization front in the case of the third type problem. The results of numerical analysis of equation (3.13) are presented in Figures 5 and 6. Note that the numerical solutions to equation (3.16) can be easy obtained from the explicit function

$$h = \frac{(u_s - u_b)e^{-\beta^2}}{\sqrt{\pi}\beta\gamma + \theta e^{-(\beta/\theta)^2}(u_b - u_0)/\mathrm{erfc}(\beta/\theta)} - \mathrm{erf}(\beta),$$

which we inverse and then plot the dependence $\beta = \beta(h)$, and from explicit function $\gamma = \gamma(\beta)$, which we inverse and then plot the dependence $\beta = \beta(\gamma)$.

Figure 5 demonstrates the typical dependencies of equation (3.13) root β (Fig. 5a) and dependencies of recrystallization front position calculated with root of equation (3.13) (Fig. 5b) on characteristic parameter of the third type problem h. It is found that β monotonically decreases with an increase in h (Fig. 5a). The width of recrystallized layer decreases with an increase in h. Therefore, the rate of recrystallization front motion decreases with a decrease in the intensity of impurity exchange between the polycrystalline and the coating. The root of equation (3.13) β monotonically decreases with an increase in γ and it increases with a decrease in θ (Fig. 6a). The kinetics of recrystallization front calculated with root of equation (3.13) is shown in Figure 6b. The rate of recrystallization in the case of $D_1 < D_2$ ($\theta > 1$) is lower than in the case of $D_1 > D_2$ ($\theta < 1$) at the fixed time.

4. CONCLUSION

We proposed two models of recrystallization taking into account the convective flux of impurity exchange between the polycrystalline and the thin-film coating. We have shown that the single-phase and two-phase Stefan problems with the boundary condition at coated surface containing the convective term can be applied to description of the special boundary modes of recrystallization.

We obtained the exact solutions of the formulated problems and analyzed in details the case of the third type problem. In was found that an increase in intensity of impurity exchange between the polycrystalline and

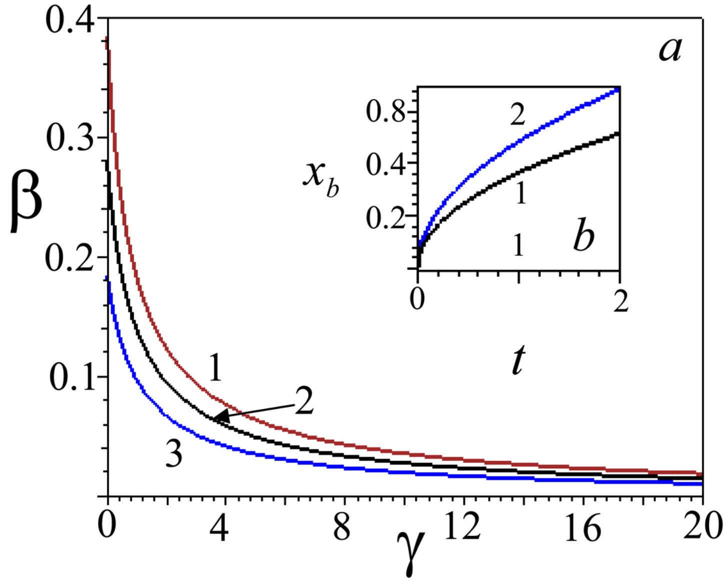

FIGURE 6. Dependencies of roots of equation (3.13) on γ (a) with $D_1 = 1$; $u_s = 1$; $u_b = 0.5$; $u_0 = 0.1$; $h = 0.5$; $\theta = 0.7$ (line 1); $\theta = 1.1$ (line 2); $\theta = 1.5$ (line 3) and the kinetic dependencies of position of recrystallization front (b) defined by (2.12) and root of equation (3.13) with $\gamma = 0.5$ and $\theta = 1.1$ (line 1); $\theta = 0.7$ (line 2) (in conventional units).

the coating promotes an increase in the width of the recrystallized layer, the rate of recrystallization, and the impurity concentration at fixed distance from the sample surface.

The results obtained supplement the theoretical concepts of the regularities of recrystallization at various boundary modes of diffusion activation [23, 32–37].

References

[1] O.M. Alifanov, Inverse Heat Transfer Problems. Springer-Verlag, Berlin (1994).

[2] N. Anento, A. Serra and Y. Osetsky, Effect of nickel on point defects diffusion in Fe-Ni alloys. *Acta Mater.* **132** (2017) 367–373.

[3] I. Apyhtina, K. Kovaleva, A. Novikov, D. Orelkina, A. Petelin and E. Yakushko, Diffusion controlled grain boundary and triple junction wetting in polycrystalline solid metal. *Defect Diffus. Forum* **363** (2015) 127–129.

[4] T. Beierling, R. Gorny and G. Sadowski, Modeling growth rates in static layer melt crystallization. *Cryst. Growth Des.* **13** (2013) 5229–5240.

[5] A.C. Briozzo and M.F. Natale, On a two-phase Stefan problem with convective boundary condition including a density jump at the free boundary. *Math. Methods Appl. Sci.* **43** (2020) 3744–3753.

[6] J. Cheng, S. Lu and M. Yamamoto, Reconstruction of the Stefan–Boltzmann coefficients in a heat-transfer process. *Inverse Prob.* **28** (2012) 045007.

[7] J. Cheng, Y. Xing, E. Dong, L. Zhao, H. Liu, T. Chang, M. Chen, J. Wang, J. Lu and J. Wan, An overview of laser metal deposition for cladding: defect formation mechanisms, defect suppression methods and performance improvements of laser-cladded layers. *Materials (Basel, Switzerland)* **15** (2022) 5522.

[8] M.V. Chepak-Gizbrekht, Modeling of grain-boundary diffusion taking into account the grain shape. *AIP Conf. Proc.* **2167** (2019) 020050.

[9] C. Evans, D. Indjin, Z. Ikonic, P. Harrison, M. Vitiello, V. Spagnolo and G. Scamarcio, Thermal modeling of terahertz quantum-cascade lasers: comparison of optical waveguides. *IEEE J. Quantum Electr.* **44**. (2008) 680-685.

[10] J. Fuller and E. Marotta, Thermal contact conductance of metal/polymer joints: an analytical and experimental investigation. *J. Thermophys. Heat Transfer* **15** (2001) 228–238.

[11] R. Ghai, K. Chen and N. Baddour, Modeling thermal conductivity of porous thermal barrier coatings. *Coatings* **9** (2019) 101.

[12] M.A. Gonik and F. Baltaretu, Problem of attaining constant impurity concentration over ingot height. *Modern Electr. Mater.* **4** (2018) 41-51.

[13] A. Gupta, V. Kulitcki, B.T. Kavakbasi, Y. Buranova, J. Neugebauer, G. Wilde, T. Hickel and S.V. Divinski, Precipitate-induced nonlinearities of diffusion along grain boundaries in Al-based alloy. *Phys. Rev. Mater.* **2** (2018) 073801.

[14] G.P. Grabovetskaya, I.P. Mishin, I.V. Ratochka, S.G. Psakhie and Yu. R. Kolobov, Grain boundary diffusion of nickel in submicrocrystalline molybdenum processed by severe plastic deformation. *Tech. Phys. Lett.* **34** (2008) 136–138.

[15] S. Herth, T. Michel, H. Tanimoto, M. Egersmann, R. Dittmar, H.-E. Schaefer, W. Frank and R. Würschum, Self-diffusion in nanocrystalline Fe and Fe-rich alloys. *Defect Diffus. Forum* **194–199** (2001) 1199–1204.

[16] R. Jendrzejewski, I. Kreja and G. Śliwiński, Temperature distribution in laser-clad multi-layers. *Mater. Sci. Eng. A* **379** (2004) 313–320.

[17] E.M. Kartashov and G.S. Krotov, Analytical solution of the single-phase Stefan problem. *Math. Models Comput. Simul.* **1** (2009) 180–188.

[18] I. Kaur, Y. Mishin and W. Gust, Fundamentals of grain and interphase boundary diffusion. Wiley, Chichester (1995).

[19] A.G. Kesarev, V.V. Kondrat'ev and I.L. Lomaev, Description of grain-boundary diffusion in nanostructured materials for thin-film diffusion source. *Phys. Metals Metallogr.* **116** (2015) 225–234.

[20] Y.R. Kolobov, G.P. Grabovetskaya, M.B. Ivanov, A.P. Zhilyaev and R.Z. Valiev, Grain boundary diffusion characteristics of nanostructured nickel. *Scr. Mater.* **44** (2001) 873–878.

[21] Yu.R. Kolobov, G.P. Grabovetskaya, K.V. Ivanov and M.B. Ivanov, Grain boundary diffusion and mechanisms of creep of nanostructured metals. *Interface Science* **10** (2002) 31–36.

[22] Y.R. Kolobov, R.Z. Valiev, G.P. Grabovetskaya *et al.*, Grain boundary diffusion and properties of nanostructured materials. Cambridge International Science Publishing, Cambridge, UK (2007), 250 p.

[23] V.V. Krasil'nikov and S.E. Savotchenko, Grain boundary diffusion patterns under nonequilibrium and migration of grain boundaries in nanoctructure materials. *Bull. Russ. Acad. Sci.: Phys.* **73** (2009) 1277–1283.

[24] Z. Li, G. Yu, X. He, S. Li, H. Li and Q. Li, Study of thermal behavior and solidification characteristics during laser welding of dissimilar metals. *Res. Phys.* **12** (2019) 1062–1072.

[25] K. Marquardt (née Hartmann), E. Petrishcheva, E. Gardés *et al.*, Grain boundary and volume diffusion experiments in yttrium aluminium garnet bicrystals at 1,723 K: a miniaturized study. *Contrib. Mineral Petrol.* **162** (2011) 739–749.

[26] H. Mehrer, Diffusion in Solids. Fundamentals, Methods, Materials, Diffusion-Controlled Processes, Springer-Verlag, Berlin, Heidelberg (2007), p. 645.

[27] A.M. Meirmanov, The Stefan Problem, Walter de Gruyter, Berlin, Germany (1992).

[28] M.F. Natale and D.A. Tarzia, Explicit solutions to the one-phase Stefan problem with temperature-dependent thermal conductivity and a convective term. *Int. J. Eng. Sci.* **41** (2003) 1685–1689.

[29] V. Niziev, F. Mirzade, V. Panchenko, M. Khomenko, R. Grishaev, S. Pityana and C. Rooyen, Numerical study to represent non-isothermal melt-crystallization kinetics at laser-powder cladding. *Model. Numer. Simul. Mater. Sci.* **3** (2013) 61–69.

[30] D. Prokoshkina, V. Esin, G. Wilde and S.V. Divinski, Grain boundary width, energy and self-diffusion in nickel: effect of material purity. *Acta Mater.* **61** (2013) 5188–5197.

[31] A.O. Rodin and A. Khairullin, Ni grain boundary diffusion in Cu-Co alloys. *Defect Diffus. Forum* **363**, (2015) 130-132.

[32] S.E. Savotchenko, Peculiarities of recrystallization activated by a diffusion flow of an impurity from a thin-film coating. *Eur. Phys. J. B* **94** (2021) 190.

[33] S.E. Savotchenko, The nonlinear wave and diffusion processes in media with a jump change in characteristics depending on the amplitude of the field distribution. *Commun. Nonlinear Sci. Numer. Simul.* **99** (2021) 105785.

[34] S.E. Savotchenko, Models of activated recrystallization on isolated grain boundaries in polycrystals. *Modern Phys. Lett. B* **36** (2022) 2150536.

[35] S.E. Savotchenko and A.N. Cherniakov, Diffusion from a constant source along nonequilibrium dislocation pipes. *Int. J. Heat Mass Transfer* **188** (2022) 122655.

[36] S.E. Savotchenko and A.N. Cherniakov The nonlinear diffusion model of recrystallization. *J. Heat Transfer* **144** (2022) 064501.

[37] S.E. Savotchenko, M.B. Ivanov and O.V. Yurova, Single-phase model of recrystallization of molybdenum activated by diffusion of nickel impurities. *Russ. Phys. J.* **50** (2007) 1118–1123.

[38] L. Shumylyak, V. Zhykharevych and S. Ostapov, Modeling of impurities segregation phenomenon in the melt crystallization process by continuous cellular automata method. *Prikladnaya diskretnaya matematika* **31** (2016) 104-118.

[39] L.N. Tao, The Stefan problem with an imperfect thermal contact at the interface. *J. Appl. Mech.* **49** (1982) 715–720.

[40] D.A. Tarzia, Exact solution for a Stefan problem with convective boundary condition and density jump. *PAMM Proc. Appl. Math. Mech.* **7** (2007) 1040307–1040308.

[41] W.A. Tiller, K. Jackson, J.W. Rutter and B. Chalmers, The redistribution of solute atoms during the solidification of metals. *Acta Metall.* **1** (1953) 428–437.

[42] C. Wang, M. He, X. Liua and J.A. Malen, Modeling the tunable thermal conductivity of intercalated layered materials with three-directional anisotropic phonon dispersion and relaxation time. *J. Mater. Chem. C* **10** (2022) 11686–11696.

[43] T. Wei, Uniqueness of moving boundary for a heat conduction problem with nonlinear interface conditions. *Appl. Math. Lett.* **23** (2010) 600–604.

[44] Y. Xian, P. Zhang, S. Zhai, P. Yang and Z. Zheng, Re-estimation of thermal contact resistance considering near-field thermal radiation effect. *Appl. Therm. Eng.* **157** (2019) 113601.

[45] G. Yang, M. Yamamoto and J. Cheng, Heat transfer in composite materials with Stefan–Boltzmann interface conditions. *Math. Methods Appl. Sci.* **31** (2008) 1297–1314.

[46] L. Zhuo, D. Lesnic and S. Meng, Reconstruction of the heat transfer coefficient at the interface of a bi-material. *Inverse Prob. Sci. Eng.* **28** (2020) 374–401.